

Origin of deep subgap states in amorphous indium gallium zinc oxide: Chemically disordered coordination of oxygen

S. Sallis, K. T. Butler, N. F. Quackenbush, D. S. Williams, M. Junda, D. A. Fischer, J. C. Woicik, N. J. Podraza, B. E. White Jr., A. Walsh, and L. F. J. Piper

Citation: *Applied Physics Letters* **104**, 232108 (2014); doi: 10.1063/1.4883257

View online: <http://dx.doi.org/10.1063/1.4883257>

View Table of Contents: <http://scitation.aip.org/content/aip/journal/apl/104/23?ver=pdfcov>

Published by the [AIP Publishing](#)

Articles you may be interested in

[Coplanar amorphous-indium-gallium-zinc-oxide thin film transistor with He plasma treated heavily doped layer](#)
Appl. Phys. Lett. **104**, 022115 (2014); 10.1063/1.4862320

[Surface reactivity and oxygen migration in amorphous indium-gallium-zinc oxide films annealed in humid atmosphere](#)

Appl. Phys. Lett. **103**, 201904 (2013); 10.1063/1.4829996

[Origin of subgap states in amorphous In-Ga-Zn-O](#)

J. Appl. Phys. **114**, 163704 (2013); 10.1063/1.4826895

[High performance solution-deposited amorphous indium gallium zinc oxide thin film transistors by oxygen plasma treatment](#)

Appl. Phys. Lett. **100**, 202106 (2012); 10.1063/1.4718022

[Subgap states in transparent amorphous oxide semiconductor, In-Ga-Zn-O, observed by bulk sensitive x-ray photoelectron spectroscopy](#)

Appl. Phys. Lett. **92**, 202117 (2008); 10.1063/1.2927306



Free online magazine

MULTIPHYSICS SIMULATION

[READ NOW ►](#)

The COMSOL logo, consisting of a small red and blue square icon followed by the word 'COMSOL' in a bold, sans-serif font.

Origin of deep subgap states in amorphous indium gallium zinc oxide: Chemically disordered coordination of oxygen

S. Sallis,¹ K. T. Butler,² N. F. Quackenbush,³ D. S. Williams,¹ M. Junda,⁴ D. A. Fischer,⁵ J. C. Woicik,⁵ N. J. Podraza,⁴ B. E. White, Jr.,^{3,1} A. Walsh,² and L. F. J. Piper^{3,1,a)}

¹Materials Science and Engineering, Binghamton University, Binghamton, New York 13902, USA

²Center for Sustainable Technologies and Department of Chemistry, University of Bath, Claverton Down, Bath BA2 7AY, United Kingdom

³Department of Physics, Applied Physics, and Astronomy, Binghamton University, Binghamton, New York 13902, USA

⁴Department of Physics and Astronomy, University of Toledo, Toledo, Ohio 43606, USA

⁵Materials Science and Engineering Laboratory, National Institute of Standards and Technology, Gaithersburg, Maryland 20899, USA

(Received 14 April 2014; accepted 29 May 2014; published online 11 June 2014)

The origin of the deep subgap states in amorphous indium gallium zinc oxide (a-IGZO), whether intrinsic to the amorphous structure or not, has serious implications for the development of *p*-type transparent amorphous oxide semiconductors. We report that the deep subgap feature in a-IGZO originates from local variations in the oxygen coordination and not from oxygen vacancies. This is shown by the positive correlation between oxygen composition and subgap intensity as observed with X-ray photoelectron spectroscopy. We also demonstrate that the subgap feature is not intrinsic to the amorphous phase because the deep subgap feature can be removed by low-temperature annealing in a reducing environment. Atomistic calculations of a-IGZO reveal that the subgap state originates from certain oxygen environments associated with the disorder. Specifically, the subgap states originate from oxygen environments with a lower coordination number and/or a larger metal-oxygen separation. © 2014 AIP Publishing LLC. [<http://dx.doi.org/10.1063/1.4883257>]

Amorphous In-Ga-Zn-O (a-IGZO) is a technologically important transparent amorphous oxide semiconductor (TAOS) for the production of thin film transistors (TFT).^{1–5} The superior carrier mobility of a-IGZO, $\sim 10 \text{ cm}^2 \text{V}^{-1} \text{s}^{-1}$ versus $\sim 1 \text{ cm}^2 \text{V}^{-1} \text{s}^{-1}$ in hydrogenated amorphous silicon (a-Si:H), combined with low temperature large area deposition compatibility and overall superior device stability have made a-IGZO the clear choice for n-type TFTs even when transparency is not a design consideration.^{2–4} It is known that the improved semiconducting properties of a-IGZO versus traditional covalent amorphous semiconductors (e.g., a-Si:H) are a consequence of the insensitivity to disorder of the overlap of the spherically symmetric metal s-orbitals that form the conduction band minimum (CBM) in a-IGZO.^{6–8}

a-IGZO films are known to form deep subgap states, which manifest as features above the valence band maximum (VBM), as shown by hard x-ray photoelectron spectroscopy (HAXPES).⁹ In general, the optical and electronic properties of devices that utilize a-IGZO active layers are strongly dependent on the number and type of subgap states present. In addition to the loss of transparency, these states are detrimental to the performance of a-IGZO based TFT devices. The foremost being the negative bias illumination stress (NBIS) instability, which results in a negative threshold shift.^{10–12} Moreover, the deep subgap states form a flat band above the VBM, which if intrinsic to TAOS, would seriously hinder the mobility of any holes formed.⁷

Although the importance of these states is well established, their origin is a subject of debate. Recent publications

have claimed that these subgap states are associated with structurally unrelaxed oxygen vacancies.^{13–16} Since the creation of oxygen vacancies is the conventional method of n-type doping transparent conducting oxides low temperature deposition of n-type doped a-IGZO currently seems to require trading optical transparency for electrical conductivity.⁸ However, vacancies are a vague concept in a structurally amorphous system. Recent density functional theory (DFT) studies of amorphous zinc tin oxide (a-ZTO) have also cast doubt on the role of oxygen vacancies, suggesting that deep subgap states in a-ZTO are linked to oxygen coordination.¹⁷

Here, we combine x-ray photoelectron spectroscopy (XPS) and atomistic electronic structure calculations to determine the microscopic origin of the subgap state in a-IGZO. We find the intensity of the subgap feature has a positive correlation with the oxygen content of the films, in variance with oxygen vacancy as the origin. Moreover, we demonstrate the ability to remove the subgap feature by low-temperature annealing in a reducing environment. Computational studies of stoichiometric a-IGZO display subgap features, further confirming that oxygen vacancies are not the cause of these states. Instead, the subgap feature is dependent on the local coordination of the oxygen environment. Details of the growth of the a-IGZO films under oxygen rich and deficient conditions, and the optical absorption and structural (x-ray diffraction, XRD and transmission electron microscopy, TEM) analysis are included in the supplementary material.¹⁸ Also, included are details of the ‘melt and quench’ approach and density functional theory calculations used for modeling the a-IGZO.^{19–21}

Films grown in our oxygen rich growth conditions did not display a deep subgap feature despite being amorphous.

^{a)}Electronic mail: lpiper@binghamton.edu

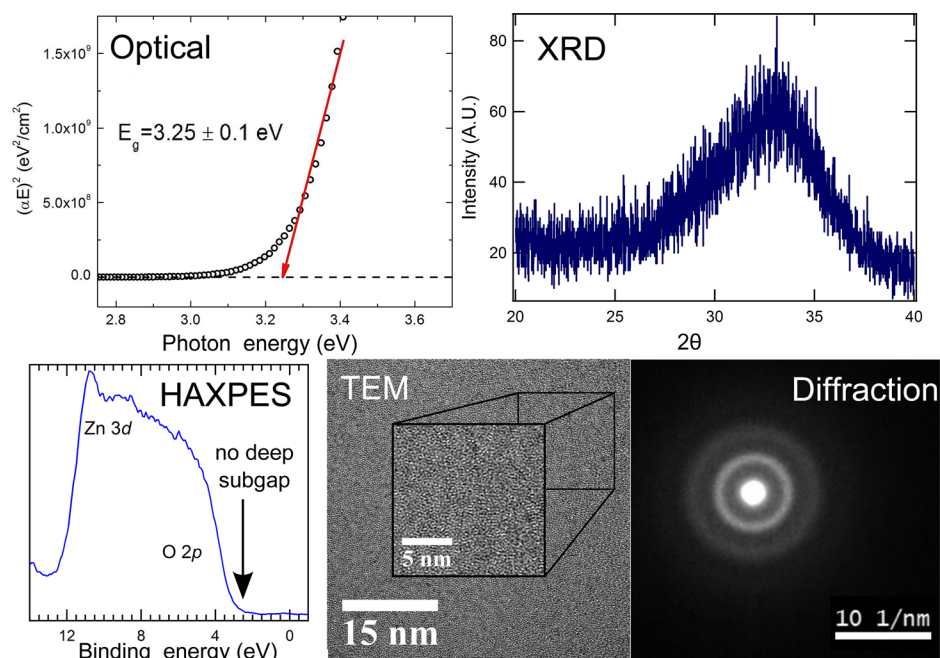


FIG. 1. The optical absorption, XRD, HAXPES, TEM, selected-area diffraction of amorphous, subgap-free a-IGZO grown in oxygen rich conditions.

Figure 1 summarizes our structural and optical results from XRD, TEM, and spectroscopic ellipsometry measurements. We note that no deep subgap feature is observed in the corresponding HAXPES for samples grown in oxygen rich conditions. These data suggest that the subgap feature is related to oxygen vacancies. However, careful compositional studies as a function of subgap evolution using XPS rule out oxygen vacancies as the origin of the deep subgap feature.

Figure 2(a) displays the valence band spectra for a-IGZO grown under oxygen-rich conditions before and after sputtering and annealing treatments to induce and manipulate the subgap feature. The spectra display the Zn 3d semi-core level and the predominately O 2p valence band. The a-IGZO films grown in these conditions were both structurally amorphous and optically transparent (i.e., no detectable subgap feature). For the as-loaded films, the valence band maximum is located approximately 3 eV below the Fermi level, with some weak band tailing between the VBM and the Fermi level. After ion sputtering, the formation of a subgap feature is observed above the VBM. The intensity of the subgap feature correlates with the degree of sputtering employed. The intensity of the induced subgap feature after the most severe sputter is comparable to the intensity of the subgap feature observed in the films grown in oxygen deficient conditions, discussed further below. Surprisingly, the complete recovery of the subgap-free state is achieved after a 15 min anneal at 200 °C in vacuum. This temperature is significantly below the crystallization temperature of a-IGZO,¹⁴ and below the glass transition temperature of most flexible polymer substrates.

The corresponding chemical compositions in Fig. 2(b) were calculated using both standard experimental sensitivity factors and a procedure to correct for the presence of adventitious carbon as per Ref. 22. As both procedures resulted in the same trends in composition vs. subgap intensity, we report only the corrected compositions. The positive correlation between oxygen composition and subgap intensity is clear. We note that the as-loaded film was oxygen deficient

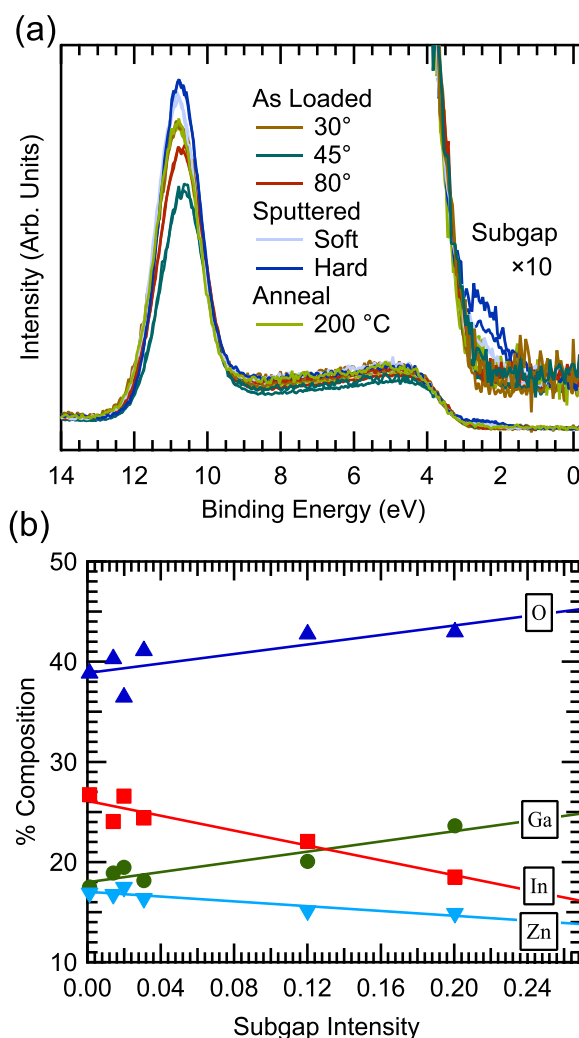


FIG. 2. (a) Valence band XPS spectra of a-IGZO sputter deposited under oxygen rich conditions and subjected to various surface treatments. The near VBM region is magnified to emphasize the changes induced in the subgap states via the surface treatments. (b) The corresponding atomic composition is plotted as a function of subgap intensity.

compared to the desired stoichiometry of the target, but showed no subgap feature. These observations combined make a compelling case for the fact that oxygen vacancies cannot be the origin of the subgap bands in the electronic density of states.

To examine this further, a larger data set of several a-IGZO samples grown on different substrates with different deposition parameters and environmental exposure was studied. To increase the signal to noise ratio of our valence band XPS spectra, without resorting to prohibitively long dwell times, we employed principle component analysis (PCA).²³ We were able to greatly enhance the signal to noise ratio in all of our valence band spectra by taking advantage of previous measurements amounting to a total of 51 valence band spectra taken over the course of two years on several a-IGZO films. The four largest eigenvectors correspond to a minimum in the embedded error, and each have a percent significance level below 10%, indicating that the spectra would be optimally reproduced by those eigenvectors.²³ The reproduction of the data using the four largest eigenvectors given by PCA is illustrated in Fig. 3(a).

The percent composition corresponding to each of the valence band spectra depicted in Fig. 3(a) was calculated

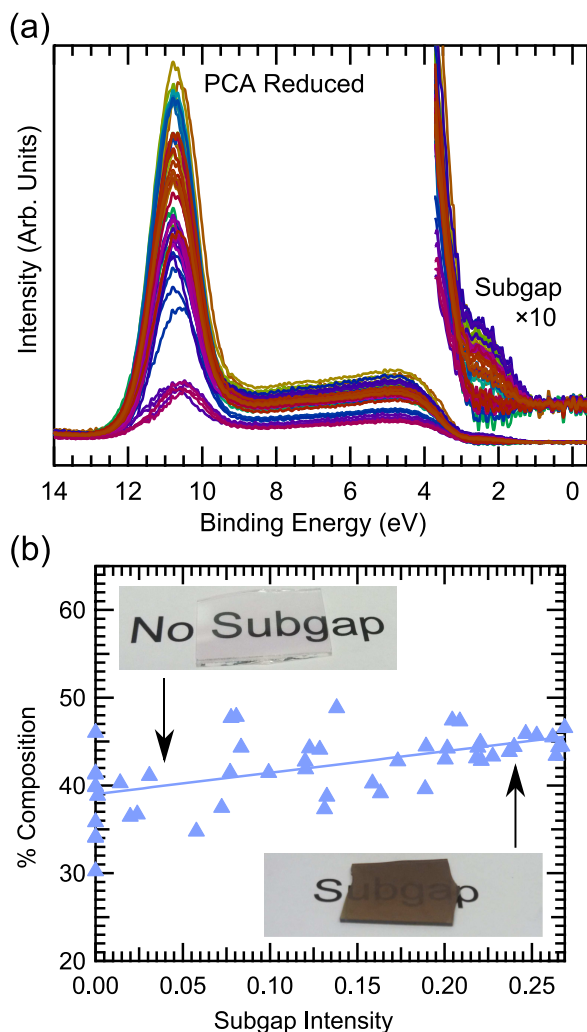


FIG. 3. (a) The PCA data reduced valence band spectra of several IGZO samples grown on different substrates with different deposition parameters and environmental exposure. (b) The corresponding oxygen composition is plotted as a function of subgap intensity.

from the core regions. All peaks in the core regions related to surface contamination and metallic precipitates were excluded from the compositional analysis. The oxygen percent composition is plotted against the normalized subgap intensity in the bottom of Fig. 3(b). The positive correlation between oxygen content and subgap intensity clearly seen in Fig. 2(b) is also apparent in this larger data set as well. This clearly indicates that the origin of the subgap feature cannot be oxygen vacancies.

In addition, similar correlations between percent composition and normalized subgap intensity for the other elemental components were observed in both data sets as well. Although oxygen vacancies cannot be the origin of the deep subgap states, the relative increase of gallium available to coordinate with the oxygen (with respect to indium) is correlated with the formation of the subgap states. Our experimental results suggest that the local environment of the oxygen sites must be important. Indeed, the observed reduction of the subgap feature with mild annealing in reducing conditions (Fig. 2) is consistent with subtle changes in the local oxygen sites.

Atomistic electronic structure calculations were performed to determine the microscopic origin of the subgap feature. The calculated band structure, and associated electronic density of states, of the stoichiometric a-IGZO composition (in some cases) contains subgap states, which confirms that oxygen vacancies are not the cause of these features. Depending on the quenching rate, localized electronic states are produced above the upper valence band, which have been confirmed to result from oxygen sites, see supplementary material for density of states plots.¹⁸ The conduction band remains unperturbed in all cases, consistent with the robust n-type conductivity. It is well known that the coordination environment of oxygen is highly sensitive to both the local and long-range electrostatic environment. This can be most succinctly described in the form of the site Madelung potential of oxygen, which for rutile and anatase structured TiO_2 has recently been shown to be the origin of the 0.4 eV valence band offset.²⁴

The distribution of the O Madelung potential, averaged over a number of amorphous structures, is compared to the layered crystalline state in Fig. 4. While the average values

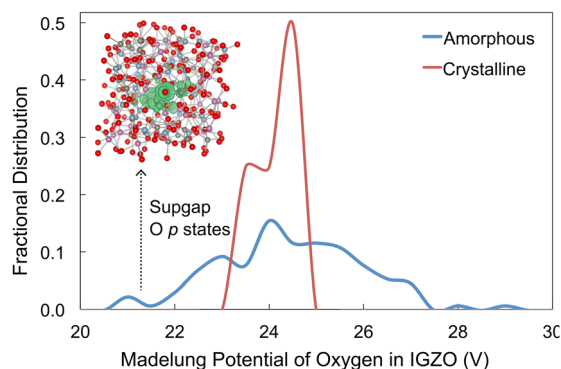


FIG. 4. The calculated distribution of the local Madelung (electrostatic) potential of oxygen in a-IGZO. Large deviation in the potential are associated with localized oxygen sites with coordination significantly perturbed from the crystalline state. Inset is the electron density associated with one such oxygen.

of the amorphous and crystalline phases are similar, the amorphous phase exhibits a much broader distribution. A larger potential results in enhanced stabilization of the O 2p states (higher binding energy), while a smaller potential correlates with a destabilization, i.e., the origin of the subgap features. The Madelung potential of an O site is largely controlled by the first coordination sphere; a lower coordination number and/or increased metal-oxygen separation result in a less-confining potential. Also shown in Fig. 4 is the real-space electron density associated with a subgap feature, which is localized on one of the O sites with the lowest electrostatic potential.

In conclusion, we have clearly demonstrated that the origin of the deep subgap feature in a-IGZO is the local coordination of the oxygen states and is not due to oxygen vacancies. Our experimental results indicate the ability to produce oxygen deficient films without necessarily producing a subgap feature. The subgap intensity can be controlled by varying the gallium content relative to indium content near the oxygen atoms. Our computational studies further disprove the role of oxygen vacancies, confirming the local coordination around the oxygen atoms as the source of the subgap feature. The local coordination of the subgap feature creates the potential for simultaneous high optical transparency and electron doping in TAOS by decoupling the intensity of the subgap feature from the oxygen deficiency of the film. Similar phenomena are expected in other functional amorphous oxide materials. Our findings provide not only a means of addressing the NBIS shift within current a-IGZO TFTs with annealing but also suggests that *p*-type TAOS may not necessarily be limited by deep subgap states.

We thank Dr. Intae Bae for assistance with the TEM measurements. L.F.J.P. gratefully acknowledges startup funding from Binghamton University and funding from the Integrated Electronics Engineering Center at the State University of New York at Binghamton. The IEEC is a New York State Center for Advanced Technology and receives funding from the New York State Foundation for Science, Technology, and Innovation (NYSTAR) as well as a consortium of industrial members. A.W. acknowledges support from the Royal Society University Research Fellowship scheme and EPSRC Grant No. EP/J017361/1. Access to the

HECToR supercomputer was facilitated through membership of the HPC Materials Chemistry Consortium (EP/F067496). The NSLS is supported by the U.S. Department of Energy, Office of Science, Office of Basic Energy Sciences, under Contract No. DE-AC02-98CH10886. Beamline X24a at the NSLS is supported by the National Institute of Standards and Technology. This material is based upon work supported by the National Science Foundation under CHE-1230246 as well as start-up funds provided by University of Toledo.

- ¹H. Ohta, K. Nomura, H. Hiramatsu, K. Ueda, T. Kamiya, M. Hirano, and H. Hosono, *Solid-State Electron.* **47**, 2261 (2003).
- ²T. Kamiya and H. Hosono, *NPG Asia Mater.* **2**, 15 (2010).
- ³T. Kamiya, K. Nomura, and H. Hosono, *Sci. Technol. Adv. Mater.* **11**, 044305 (2010).
- ⁴W. Lim, E. A. Douglas, S.-H. Kim, D. P. Norton, S. J. Pearton, F. Ren, H. Shen, and W. H. Chang, *Appl. Phys. Lett.* **93**, 252103 (2008).
- ⁵E. Fortunato, P. Barquinha, and R. Martins, *Adv. Mater.* **24**, 2945 (2012).
- ⁶R. Martins, P. Barquinha, I. Ferreira, L. Pereira, G. Gonçalves, and E. Fortunato, *J. Appl. Phys.* **101**, 044505 (2007).
- ⁷A. Walsh, J. L. F. D. Silva, and S.-H. Wei, *Chem. Mater.* **21**, 5119 (2009).
- ⁸J. E. Medvedeva and C. L. Hettiarachchi, *Phys. Rev. B* **81**, 125116 (2010).
- ⁹K. Nomura, T. Kamiya, H. Yanagi, E. Ikenaga, K. Yang, K. Kobayashi, M. Hirano, and H. Hosono, *Appl. Phys. Lett.* **92**, 202117 (2008).
- ¹⁰K. Nomura, T. Kamiya, and H. Hosono, *Appl. Phys. Lett.* **99**, 053505 (2011).
- ¹¹B. Ryu, H.-K. Noh, E.-A. Choi, and K. J. Chang, *Appl. Phys. Lett.* **97**, 022108 (2010).
- ¹²H. Oh, S.-M. Yoon, M. K. Ryu, C.-S. Hwang, S. Yang, and S.-H. K. Park, *Appl. Phys. Lett.* **97**, 183502 (2010).
- ¹³H. Omura, H. Kumomi, K. Nomura, T. Kamiya, M. Hirano, and H. Hosono, *J. Appl. Phys.* **105**, 093712 (2009).
- ¹⁴K. Ide, K. Nomura, H. Hiramatsu, T. Kamiya, and H. Hosono, *J. Appl. Phys.* **111**, 073513 (2012).
- ¹⁵T. Kamiya, K. Nomura, and H. Hosono, *Phys. Status Solidi A* **207**, 1698 (2010).
- ¹⁶H.-K. Noh, K. J. Chang, B. Ryu, and W.-J. Lee, *Phys. Rev. B* **84**, 115205 (2011).
- ¹⁷W. Körner, P. Gumbsch, and C. Elsässer, *Phys. Rev. B* **86**, 165210 (2012).
- ¹⁸See supplementary material at <http://dx.doi.org/10.1063/1.4883257> for details of optical and structural properties of the amorphous O rich samples, and the density of states calculations.
- ¹⁹J. D. Gale and A. L. Rohl, *Mol. Simul.* **29**, 291 (2003).
- ²⁰G. Kresse and J. Furthmüller, *Phys. Rev. B* **54**, 11169 (1996).
- ²¹G. Kresse and J. Furthmüller, *Comput. Mater. Sci.* **6**, 15 (1996).
- ²²S. Evans, *Surf. Interface Anal.* **25**, 924 (1997).
- ²³E. R. Malinowski, *Factor Analysis in Chemistry* (Wiley, 1991).
- ²⁴D. O. Scanlon, C. W. Dunnill, J. Buckeridge, S. A. Shevlin, A. J. Logsdail, S. M. Woodley, C. R. A. Catlow, M. J. Powell, R. G. Palgrave, I. P. Parkin *et al.*, *Nature Mater.* **12**, 798 (2013).